AFCRL-70-0091

Statistical Band Model Parameters and Integrated Intensities for the 5.9μ, 7.5μ, and 11.3μ Bands of HNO_3 Vapor

Aharon Goldman, Thomas G. Kyle

Department of Physics, University of Denver, Denver, Colorado 80210

and

Francis S. Bonomo

Department of Chemistry, University of Denver, Denver, Colorado 80210

Contract: F19628 68-C-0233

Project No. 8662

SCIENTIFIC REPORT No. 7

January 1970

This research was sponsored by the Advanced Research Projects Agency under ARPA Order No. 36?

Contract Monitor: Robert McClatchey
Optical Physics Laboratory

Prepared for

Air Force Cambridge Research Laboratories

Office of Aerospace Research

United States Air Force

Bedford, Massachusetts 01730

AFCRL-70-0091

Statistical Band Model Parameters and Integrated Intensities for the 5.9μ, 7.5μ, and 11.3μ Bands of HNO_3 Vapor

Aharon Goldman, Thomas G. Kyle

Department of Physics, University of Denver, Denver, Colorado 80210

and

Francis S. Bonomo

Department of Chemistry, University of Denver, Denver, Colorado 80210

Contract: F19628-68-C-0233

Project No. 8662

SCIENTIFIC REPORT No. 7

January 1970

This research was sponsored by the Advanced Research Projects Agency under ARPA Order No. 363

Contract Monitor: Robert McClatchey
Optical Physics Laboratory

Prepared for

Air Force Cambridge Research Laboratories

Office of Aerospace Research

United States Air Force

Bedford, Massachusetts 01730

ABSTRACT

Quantitative absorption measurements of the 5.9μ, 7.5μ and the 11.3μ bands of pure HNO_3 vapor were carried out at 40°C. Use was made of absorption cells of various lengths in order to obtain curves of growth. The statistical spectral band model was applied and band model parameters and integrated intensities were derived.

TABLE OF CONTENTS

LIST OF FIGURES

LIST OF FIGURES Cont.

Figure No.

LIST OF TABLES

1. INTRODUCTION

Nitric acid has often been suspected of playing a role in air pollution processes,[1] but more recently it has been found to be present in the atmosphere above 20 kilometers altitude.[2] Its presence was discovered by means of infrared absorption, and this appears to be the method which will be involved in future studies of its atmospheric distribution. The amounts of nitric acid involved in the originally reported experiments have been determined by laboratory measurements which duplicated the reported absorptions.[3] The present results indicate that these estimates of the amount present in the atmosphere might be too large.

This study was carried out to enable future atmospheric data to be interpreted without the need to return to the laboratory with each new piece of data. This can be accomplished by the use of the absorption parameters based upon the statistical model of the different absorption bands. In fact, this molecule is very well suited to the model by its very large number of closely spaced lines.

The nitric acid molecule is a nearly planar molecule. Its normal modes of vibration have previously been determined, and assigned to the different bands.[4] There are four strong bands located at 5.9μ, 7.5μ, 11.3μ and 22μ, but only the first three are reported in this study. Only self-broadening is considered. It was originally planned to examine nitrogen broadening also, but it was found that with the cell lengths available, the change in the absorption produced by pressurizing with nitrogen was very

small, in comparison to the unpressurized absorption. This would have prevented an accurate determination of the relative broadening effect of nitrogen.

The nitric acid molecule, because of its size, might be expected to be much more effective in line broadening than nitrogen. This is still thought to be so. The reason the effects of nitrogen could not be seen clearly was due to the very close spacing of the lines in the bands. As soon as there is any significant pressure, the width of the lines is large enough to make them almost completely overlapping.

2. THE STATISTICAL SPECTRAL BAND MODEL METHOD

The present measurements were made with pure HNO_3 vapor only. According to the spectral band model for a pure gas, the mean spectral transmittance $\bar{T}(\nu)$ of a statistical array of Lorentz lines is determined by two basic parameters $\alpha(\nu)$ (cm^{-1}) and $\beta(\nu)$ (atm^{-1}):

$$\alpha(\nu) = x(\nu)/L = S^{o}(\nu)/2\pi\gamma^{o}(\nu) \quad , \tag{1a}$$

$$\beta(\nu) = 2\pi\gamma^{o}(\nu)p/d(\nu) = \beta^{o}(\nu)p \quad . \tag{1b}$$

Here $x(\nu)$ is the dimensionless Ladenburg-Reiche parameter, $S^{o}(\nu)$ (cm^{-2} atm^{-1}) is the mean line intensity at unit pressure, $\gamma^{o}(\nu)$ (cm^{-1} atm^{-1}) is the mean halfwidth of the lines at unit pressure, $d(\nu)$ (cm^{-1}) is the mean spacing between the lines, $p(atm)$ is the pressure and $L(cm)$ is the path length.

The mean transmittance is given by

$$\bar{T}(\nu) = \exp[-\bar{W}(\nu)/d(\nu)] \quad , \tag{2}$$

where $\bar{W}(\nu)$ is the value of the equivalent width, averaged over the line intensity distribution function $P(S(\nu))$:

$$\bar{W}(\nu) = \int_{0}^{\infty} W(S(\nu),\beta(\nu))P(S(\nu))dS \tag{3}$$

Assuming equally intense lines, i.e., $P(S(\nu)) = \delta(S(\nu)-S_{o}(\nu))$ where $S_{o}(\nu)$ represents the average intensity, $\bar{T}(\nu)$ can be expressed in terms of a single Lorentz line:

$$\bar{T}(\nu) = \exp[-\beta(\nu)f(\alpha(\nu)L)] \quad , \tag{4}$$

where f(x) is the Ladenburg-Reiche function:

$$f(x) = x \exp(-x)[I_o(x) + I_1(x)] \quad , \tag{5}$$

where I_o and I_1 are modified Bessel functions.

A more realistic and convenient intensity distribution function is given by the exponential distribution: $P(S(\nu)) = \exp(-S(\nu)/S_o(\nu))$. A simple expression is then derived for $\bar{T}(\nu)$:

$$\bar{T}(\nu) = \exp\left\{-\frac{\alpha(\nu)\beta^o(\nu)pL}{[1+2\alpha(\nu)L]^{\frac{1}{2}}}\right\} \quad . \tag{6}$$

Several other intensity distribution functions have been recently discussed in the literature,[5] such as the exponential tailed S^{-1} line intensity distribution $P(S(\nu)) \propto S^{-1}(\nu)\exp[-S(\nu)/S_o(\nu)]$ for which the statistical model gives

$$\bar{T}(\nu) = \exp\left\{-(\beta^o(\nu)p/4)[(1+8\alpha(\nu)L)^{\frac{1}{2}}-1]\right\} \quad . \tag{7}$$

The plot of $\bar{W}(\nu)/\beta(\nu)$ against $x(\nu)$ defines a spectral "curve of growth", having "linear" and "square root" regions. These regions are given by the limiting form of $\bar{W}(\nu)/\beta(\nu)$ for $x \ll 1$ and $x \gg 1$, respectively. If f(x) is transformed according to $(\pi/4)f(4x/\pi)$ the three line intensity distribution functions mentioned above yield the same asymptotes for the corresponding curves of growth: x and $(x/2)^{\frac{1}{2}}$ for $x \ll 1$ and $x \gg 1$, respectively. However, they differ in curvature in the central region. The curvature of $\bar{W}(\nu)/\beta(\nu)$ from Eq.(7) is smaller than that from Eq.(6) which in turn is smaller than that from Eq.(5).

For the application of the band model to experimental measurements it is fundamental that the quantity $-(\ell n\bar{T}(\nu))/p$, for a given

path length and temperature, must be independent of pressure when the statistical model of Lorentz lines is valid. (For low enough pressures, $-(\ell n\, \bar{T}(\nu)/p$ will increase with decreasing p, indicating Doppler broadening.) Thus measurements over a large range of path length and pressures are carried out, and for each path length L_j the average value $y_j(\nu) = \left[-(\ell n\, \bar{T}(\nu,L_j))/p\right]_{av}$ is derived. By plotting $y_j(\nu)$ against L_j the "curve of growth" can be obtained.

As shown in Fig. 3 of Ref. 6, the differences between the different curves of growth with different line intensity distributions in the central region range from 10% to 20%. The experimental error in $y_j(\nu)$ is generally about $\pm 5\%$. Therefore, the effect of the different line intensity distribution on the curves of growth can generally be observed, even though the results for the band model parameters $\alpha(\nu)$, $\beta^o(\nu)$ will not be extremely changed. In particular, $S^o(\nu)/d(\nu)$ will be practically unaffected since it is independent of the line intensity distribution.[6]

The curve fitting may be done (for each frequency) graphically, by shifting vertically and horizontally the experimental plot of $y_j(\nu)$ against L_j over a theoretical plot of $\bar{W}(\nu)/\beta(\nu)$ against $x(\nu)$, both on a log-log scale, until coincidence of the two curves occurs. It is easily shown that the point of intersection of the asymptotes of $\bar{W}(\nu)/\beta(\nu)$ has an abcissa L_o(cm) which satisfies the relation

$$\alpha(\nu) = 1/(2L_o) \quad . \tag{8}$$

The ordinate of this intersection is $y_o(atm^{-1})$ which satisfies

$$\beta^o(\nu) = 2y_o \qquad (9)$$

and thus the band model parameters, $\alpha(\nu)$ and $\beta^o(\nu)$, are determined. It should be noted that this graphical method is similar to the method for deriving S^o and γ^o of a single line described by Benedict et al.[7]

In using the graphical method it is important to have measurements over a range of path length such that the asymptotic regions to the "curves of growth" are obtained, otherwise the resulting error may be quite large due to the log-log scale on which the fitting is made. Additional points in the central region will determine the nature of the line intensity distribution.

Computerized methods can also be used for optimal fitting of the experimental points to the "curves of growth". A simple least square fitting is not possible because the functions involved are not linear in the parameters $\alpha(\nu)$, $\beta^o(\nu)$. In the case of exponential intensity distribution, (Eq.(6)), the fitting may be done by minimizing the expression[8]

$$\Sigma_j [1 + b(\nu)\, L_j - a(\nu)\, L_j^2 / y_j^2(\nu)]^2 \quad , \qquad (10)$$

where $a(\nu) = \alpha^2(\nu)\beta^2(\nu)$ and $b(\nu) = 2\alpha(\nu)$. Here the fitting is made for <u>relative</u> changes in y_j rather than for y_j itself, in order to allow the same weight for every change of y_j. The absolute change in y_j will give a greater weight to a greater y_j (which can be several orders of magnitude greater than a smaller one).

This type of fitting is not possible for the exponential tailed S^{-1} intensity distribution. In this case the fitting can be done by an iterative procedure described in a previous paper.[9] It is based on the minimalization of the expression

$$\Sigma_j \Big[\Delta y_j(\nu)/y_j(\nu) - \frac{\partial F}{\partial \alpha(\nu)} (\alpha(\nu),\beta^o(\nu),L_j)\Delta\alpha(\nu)/y_j(\nu) - \frac{\partial F}{\partial \beta^o(\nu)} (\alpha(\nu),\beta^o(\nu),L_j)\Delta\beta^o(\nu)/y_j(\nu)\Big]^2 , \quad (11)$$

where $F(\alpha(\nu),\beta^o(\nu),L_j)$ is the theoretical expression for $y_j(\nu)$, the consecutive iterations are made by

$$\alpha(\nu)_{i+1} = \alpha(\nu)_i + \Delta\alpha(\nu) \quad , \quad (12a)$$

$$\beta^o(\nu)_{i+1} = \beta^o(\nu)_i + \Delta\beta^o(\nu) \quad , \quad (12b)$$

and the convergence condition is taken as

$$|\Delta\alpha(\nu)/\alpha(\nu)| + |\Delta\beta^o(\nu)/\beta^o(\nu)| < \epsilon \quad . \quad (13)$$

The iteration method can be used for other functions, arising from different intensity distributions. The convergence is very fast: for most practical cases not more than 5 iterations are needed for $\epsilon = 0.0002$.

The results for $\alpha(\nu)$, $\beta^o(\nu)$ may be used for determination of the mean transmittance of a pure gas (by inserting the band model parameters into the mean transmittance equation) and also for a gas mixture. In the latter case, the transmittance equation takes on somewhat different form.

The line halfwidth γ_m for a binary gas mixture, with partial pressures p_a (absorber) and p_f (foreign) depends on pressure according to the relation:

$$\gamma_m = \gamma_m^o \, p_e \quad , \tag{14}$$

where γ_m^o is the line halfwidth at unit pressure (cm^{-1} atm^{-1}) characteristic of the specific gas mixture, and p_e is the equivalent pressure defined by

$$p_e = p_f + Bp_a = p_t + (B-1)p_a \quad , \tag{15}$$

where B is the broadening coefficient, and p_t is the total pressure.

An equivalent path length L_e (cm) is now defined by

$$L_e = (p_a/p_e)L \quad . \tag{16}$$

By using p_e, L_e $B\alpha(\nu)$, $\beta^o(\nu)/B$ instead of p, L, $\alpha(\nu)$, $\beta^o(\nu)$, the transmittance equation can be used for the specific gas mixture. For example, Eq.(6) will take the form

$$\bar{T}(\nu) = \exp\left\{\frac{-\beta^o(\nu)\alpha(\nu)p_e L_e}{[1 + 2\alpha(\nu)B\,L_e]^{\frac{1}{2}}}\right\} \quad . \tag{17}$$

The band model parameters can also be used for the determination of integrated intensities. The integrated intensity of an absorption band is given by

$$S_b^o = \int_{band} k(\nu)d\nu \quad , \tag{18}$$

where $k(\nu)$ is the spectral absorption coefficient. Two methods can be used to derive S_b^o. One is to integrate the product $\alpha(\nu)\beta^o(\nu)$

over the band. This is justified by the fact that $\alpha(\nu)\beta^{o}(\nu) = S^{o}(\nu)/d(\nu)$ gives the absorption coefficient $k(\nu)$ and therefore

$$S_b^o = \int_{band} (S^o(\nu)/d(\nu))d\nu \quad . \tag{19}$$

The other method is to integrate $-(\ell n\ T(\nu))/pL$ over the band for a cell for which the absorption is in the linear region, where

$$\bar{T}(\nu) \approx \exp[-(S^o(\nu)/d(\nu))pL] \quad , \tag{20}$$

and thus

$$S_b^o = -\frac{1}{pL} \int_{band} (\ell n\ \bar{T}(\nu))\, d\nu \quad . \tag{21}$$

The accuracy of the first method is in general much better than that of the second. This is because random errors are corrected during the curve fitting process.

3. EXPERIMENTAL

Anhydrous nitric acid was prepared by low pressure distillation from a sulfuric acid mixture in the apparatus shown in Fig. 1. Reagent grade concentrated nitric acid, (70% HNO_3) manufactured by DuPont, was used as the source for the HNO_3 vapor. Reagent grade concentrated sulfuric acid, manufactured by DuPont, was used as dehydrating agent. In Fig. 1 A is a 100 ml. Pyrex glass distillation flask, topped with a simple distillation head and thermometer B. The receiver C is a 200 ml glass trap immersed in liquid nitrogen. Pressure was measured with a McLeod gauge, and the vacuum pump F was protected from acidic gases by a trap E, which contained about 200 grams of soda-lime. Ball and socket joints, size 18/9, were used between elements of the apparatus to facilitate disassembly and cleaning. Halocarbon grease (type #25-5S, Halocarbon Products Corporation) was used to lubricate and seal the ball joints and vacuum stopcocks. This grease is not affected by nitric acid vapor, nitrogen oxides, or other oxidizing gases.

Distillation was carried out at a pressure of about 30 microns from a mixture of nitric and sulfuric acids prepared in the ratio of one volume of nitric to 1.4 volumes of sulfuric acid. This ratio gives a stoichiometric ratio of one molecule of water (from the nitric acid) to one molecule of sulfuric acid forming the mono-hydrated acid. Usually a slight excess (5%) of sulfuric acid was added to the mixture, which typically was made up of 25 ml nitric acid and 35 ml sulfuric acid.

When the sample was not in use, it was stored in the evacuated receiver at liquid nitrogen temperature. When stored in this manner, the acid remained colorless for several weeks; when stored at $0^{\circ}C$. for four days, it began to turn slightly yellow.

To be sure that a single distillation was effective in producing pure anhydrous nitric acid, a batch of singly distilled acid was redistilled from sulfuric acid. Spectra of the two products were identical. This doubly distilled acid was used for most of the experiments reported here.

The apparatus used for handling the nitric acid vapor is shown in detail in Fig. 2. Since it is a glass system and nitric acid vapor is photochemically decomposed, the work was performed with subdued incandescent illumination. The cold sample receiver A from the distillation apparatus (wrapped in aluminum foil to exclude light) was attached to the apparatus at a point near the infrared gas cell B. Vacuum was obtained from the pump J, protected by traps of liquid nitrogen H, and soda-lime I. Ultimate pressure in the system was measured with a McLeod gauge. When nitric acid was in the system the McLeod gauge was blocked off to protect the mercury. Pressures of nitric acid were read with either of two manometers; one, G, a standard mercury-filled manometer with a 1/2 inch layer of Kel-F (Minnesota Mining & Manufacturing Co., Grade KF-3) halocarbon oil on the surface to protect the mercury, the other, F, a differential manometer filled with the same oil. Nitrogen gas could be admitted (through a phosphorus pentoxide drying tube, C) for pressure broadening experiments or for sweeping the system out.

Infrared spectra were made with a Beckman Model IR-7 spectrophotometer. This is a double-beam NaCl-foreprism grating instrument with a range from 600 to 4000 cm^{-1}, and is purged with dried air. Four gas cells were used, two commercial and two built in the laboratory. The two commercial cells were 10 and 5 cm Pyrex glass cells obtained from Wilks Scientific Corp. These were equipped with Teflon stopcocks and silicone o-rings. The silicone o-rings were readily attacked by nitric acid as evidenced by the gradual appearance in the HNO_3 spectrum of several absorption features, the strongest being at 1095 cm^{-1}. These bands were identified as characteristic of alkoxy-silanes, derived from the silicone polymer. These o-rings were replaced with Viton which showed no deterioration after considerable use. The o-rings were greased lightly with halocarbon grease. The windows were AgCl, 1/4" thick by 2" diameter. Assembled path lengths were 99.40 and 49.30 mm.

The laboratory-built gas cells are shown in detail in Fig. 3. These cells had path lengths of 10.20 and 20.28 mm, were built to accommodate the 1/4" thick by 2" diameter AgCl windows, and were inert to the nitric acid vapor. Unfortunately, the very narrow inside diameter of the glass inlet tubing (1/16") permitted only slow diffusion when pressure broadening experiments were carried out. As with the long path cells the only materials in contact with the acid vapor were glass, Teflon, halocarbon grease, Viton, and AgCl.

It was observed during the course of handling the silver chloride windows, that when a window had a strongly reduced surface

resulting in a silver mirror, this mirror was subject to reaction with the anhydrous HNO_3. This resulted in deposits of nitrate salts and removal of the mirror. It was found that such mirrors could be avoided in advance of use as a cell window by soaking for several minutes in concentrated nitric acid.

Temperature of the gas samples while spectra were being taken was $40^{\circ}C \pm 2^{\circ}C$. Resolution for the quantitative spectra was about 10 cm^{-1}, while that for the high resolution scans was ~ 0.5 cm^{-1}.

4. MEASUREMENTS AND RESULTS

In order to examine the purity of the HNO_3 vapor sample and to select the appropriate spectral model of the bands, preliminary spectra with ~0.5 cm^{-1} resolution were first recorded. The observed spectra, in which rotational lines could not be resolved, show the "statistical" nature of the HNO_3 spectrum. Such a spectrum is shown in Fig. 4. The identification of the different HNO_3 bands is according to McGraw et al.[4] The only impurity that could be identified in the spectra is the ν_3 band of NO_2 near 1618 cm^{-1}. The integrated intensity of this band is quite large[10] - 2059 (cm^{-2} atm^{-1}) at 25°C - which is about twice the intensity of the strongest HNO_3 band (see below). In view of the small absorption present due to this band, it was estimated that the NO_2 impurity introduces only a small error of about 1% in the pressure measurements for HNO_3.

For measurements of the mean transmittance $\bar{T}(\nu)$ the geometrical slit width of the spectrometer was increased to 0.50 mm, corresponding to a spectral slit width of about 10 cm^{-1}. Absorption spectra were taken with the four cells. For a given cell spectra were recorded for a series of different pressures, from 8 to 12 pressures for each cell. The pressure ranged from 1 mm Hg in the longest cell (99.4 mm) to 65 mm Hg in the shortest cell (10.2 mm). The measurements procedure was as follows. The envelope, with the cell in vacuum (~10 micron) was recorded first. Then different pressures were introduced, by admitting fresh HNO_3 vapor to the cell for each run. The pressures were chosen so that the peak

absorption varied between 20% and 80%, in order to minimize the error[11] in dariving $-\ell n\, \bar{T}(\nu)$. Only the three regions of interest were recorded during the runs with the different pressuras, except in the last run with the highest pressure in which the complete region from 600 to 4000 cm^{-1} was racorded. The final step was to evacuate the cell and to again record the base-lina. In ganaral, the second base-line was made about 4 hours after the first one and it was found to agree with the first one within $\pm 0.5\%$. Typical spectra obtained according to this procedure with tha 49.3 mm cell are reproduced in Fig. 5.

The mean transmittance was determined from tha racorded spectra for many frequancies - about 30 frequancias for each band - at 2.5 cm^{-1} intervals. The salected net of frequencias follows closely the shapa of the transmittance curve. For aach selactad frequency $-(\ell n\, \bar{T}(\nu))/p$ was than calculated. It was found that for a given call langth and fraquency, the quantity $-(\ell n\, \bar{T}(\nu))/p$ was indepandant of prassure to within $\pm 4\%$ with tha exception of few measurements at low pressures (below 3 mm Hg) for which deviations up to 20% from the average wera obsarved. Tha constancy of $-(\ell n\, \bar{T}(\nu))/p$ as a function of p for pressuras abova 3 mm Hg proves the validity of the statistical modal with Lorentz line shape. However, it is not obvious if the deviations at low pressures are due to Doppler broadening or due to axperimental error in the determination of the low pressuras of HNO_3 vapor. Excluding the few low prassure measurements, the avarage values

$y_j(\nu) = [-(\ell n\ \bar{T}(\nu))/p]_{av}$ were then obtained (one for each cell). A typical example of the deviation of $-(\ell n\ \bar{T}(\nu))/p$ from the average as a function of p is shown in Fig. 6 for $\nu = 1700\ cm^{-1}$ in the 49.3 mm cell. In this example, the point at 2.5 mm Hg was excluded from the average.

The resulting average values of $y_j(\nu)$ were then fitted to the statistical band model. Results for the band model parameters $\alpha(\nu) = x(\nu)/L, \beta^o(\nu) = 2\pi\gamma^o(\nu)/d(\nu)$ and their product $S^o(\nu)/d(\nu)$ are given in Tables I.-III. The values of $S^o(\nu)/d(\nu)$ are also plotted against ν for the three bands under consideration in Figs. 7-9. The parameters are defined for unit pressure (1 atm) at the temperature of the experiment (40°C). These parameters were derived for an exponential line intensity distribution, i.e., according to Eq.(6), using the least square procedure outlined in Eq.(10). The results show that $x(\nu)/L < 0.05$ so that the experimental points fall in the linear and in the central region of the curves of growth. Even the 99.4 mm cell was not long enough to achieve the square root region. Therefore, it is expected that the errors in $\alpha(\nu)$ and $\beta^o(\nu)$ are much larger than the error in $S^o(\nu)/d(\nu)$. The experimental points were also fitted to an exponential line intensity distribution, using the iteration procedure, and to an exponential tailed S^{-1} line intensity distribution using the iteration procedure. Also, the experimental points were arbitrarily changed by ±5% and then fitted in the same way as in Tables I.-III. No improvement in the fitting was obtained by using the exponential tailed S^{-1} line intensity distribution. The fitting to this model did not have

a significant influence on $S^o(\nu)/d(\nu)$, but values for $\alpha(\nu)$ and $\beta^o(\nu)$ differed by up to 50%. An error estimate could be obtained from the different fitting procedures used, typical results for which are shown in Table IV. for $\nu = 1700\ cm^{-1}$. It is estimated that the average errors in $\alpha(\nu)$,$\beta^o(\nu)$ are ~50% while the error in $S^o(\nu)/d(\nu)$ is ~5%.

Since Tables I.-III. can be regarded as representing the values of $x(\nu)$ for a 1-cm path length, it is clear that for a 1-cm path length all mean transmittance values follow Lambert-Beer's law:

$$\bar{T}(\nu) = \exp[-k(\nu)pL] \quad , \tag{22}$$

where

$$k(\nu) = \alpha(\nu)\beta^o(\nu) = S^o(\nu)/d(\nu) \quad . \tag{23}$$

On the other hand, for most frequencies, path lengths greater than ~10 cm no longer give results which lie in the linear region of the curve of growth. The assumption of Lambert-Beer's law may then lead to serious errors.

Integrated intensities for the three bands were derived as shown in Table V. The two methods mentioned above were used to derive the integrated intensities - one by $\int \alpha(\nu)\beta^o(\nu)d\nu$ and the other by $\int -\ell n\, T(\nu)d\nu/pL$ (see Eqs. (19), (21)). The second method was applied to the shortest cell (10.28 mm), for which $x(\nu)<0.05$ which is well in the linear region of the curve of growth. However, according to the discussion in the previous section, the values of $\int\alpha(\nu)\beta^o(\nu)d\nu$ are regarded as the best values for the integrated intensities. With the error limits quoted in Table V. both methods gave consistent results.

REFERENCES

1. P. A. Leighton, Photochemistry of Air Pollution (Academic Press, New York, 1961).

2. D. G. Murcray, T. G. Kyle, F. H. Murcray, and W. J. Williams, J. Opt. Soc. Am. 59, 1131 (1969).

3. P. E. Rhine, L. D. Tubbs, and D. Williams, J. Opt. Soc. Am. 59, 483 (1969); Appl. Opt. 8, 1500 (1969)

4. G. E. McGraw, D. I. Bernitt, and I. C. Hisatsune, J. Chem. Phys. 42, 237 (1965).

5. W. Malkmus, J. Opt. Soc. Am. 57, 323 (1967).

6. A. Goldman, and T. G. Kyle, Appl. Opt. 7, 1167 (1968).

7. W. S. Benedict, R. Herman, G. E. Moore, and S. Silverman, Can. J. Phys. 34, 830,850 (1956).

8. A. Goldman, J. Quant. Spectr. Radiat. Transfer 8, 829 (1968).

9. A. Goldman, E. Finkman and U. P. Oppenheim, J. Opt. Soc. Am. 59, 1218 (1969).

10. A. Guttman, J. Quant. Spectr. Radiat. Transfer 2, 1 (1962).

11. H. K. Hughes, Appl. Opt. 2, 1937 (1963).

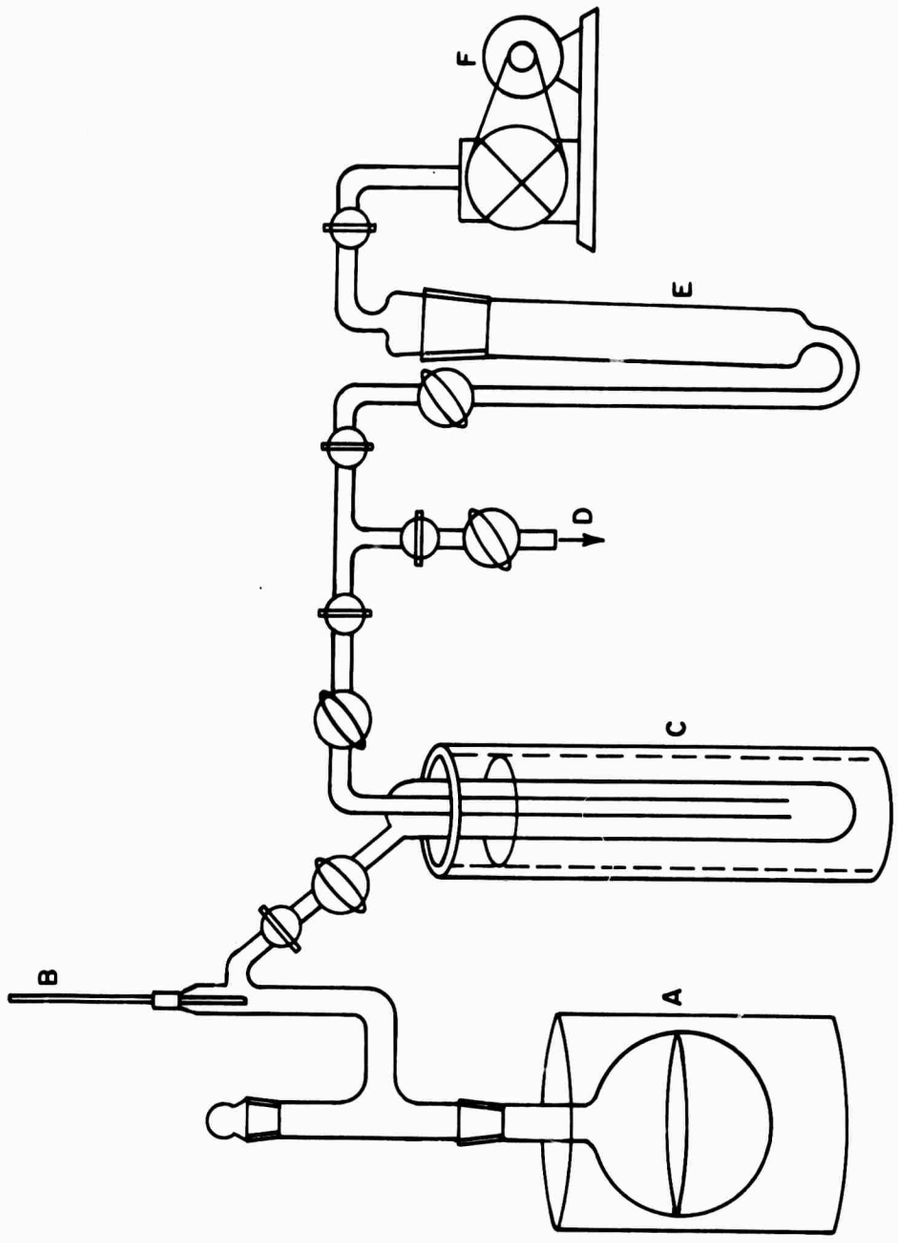

Fig. 1. Schematic diagram of the apparatus for the purification of HNO_3.

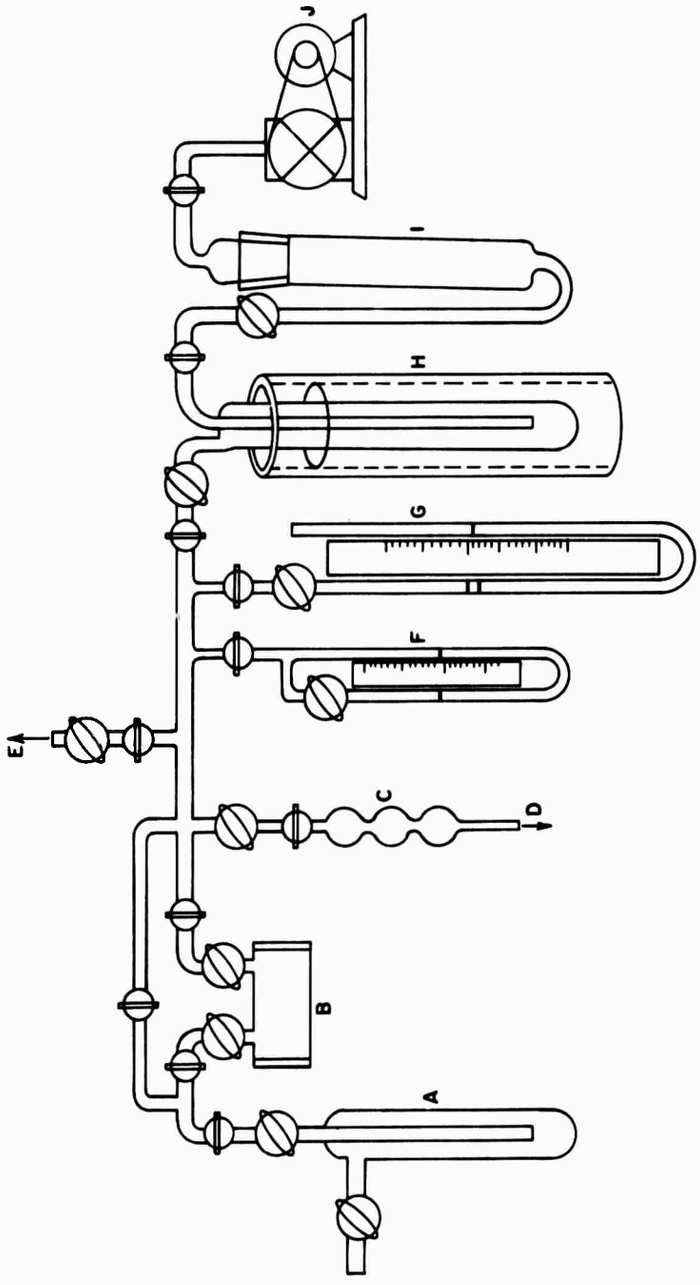

Fig. 2. Schematic diagram of the gas handling system.

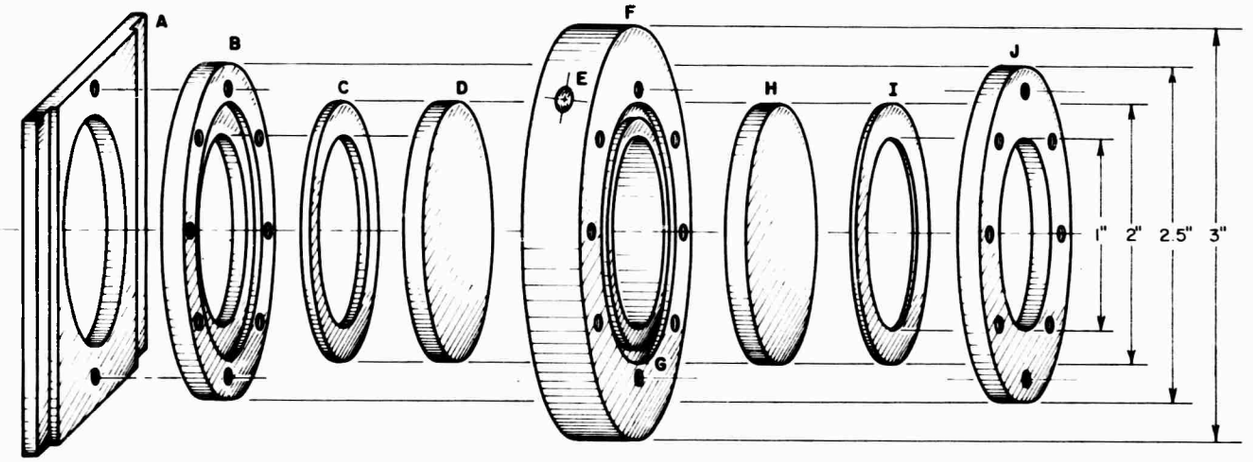

Fig. 3a. Schematic diagram of the Teflon absorption cell.

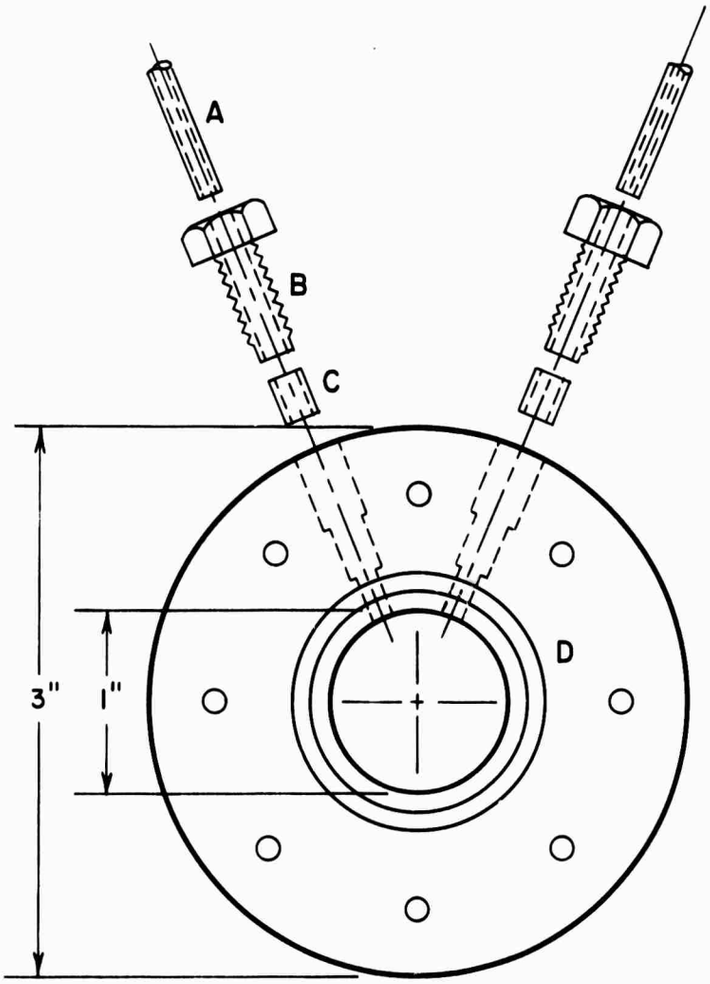

Fig. 3b. Schematic diagram of the cross section of the cell body.

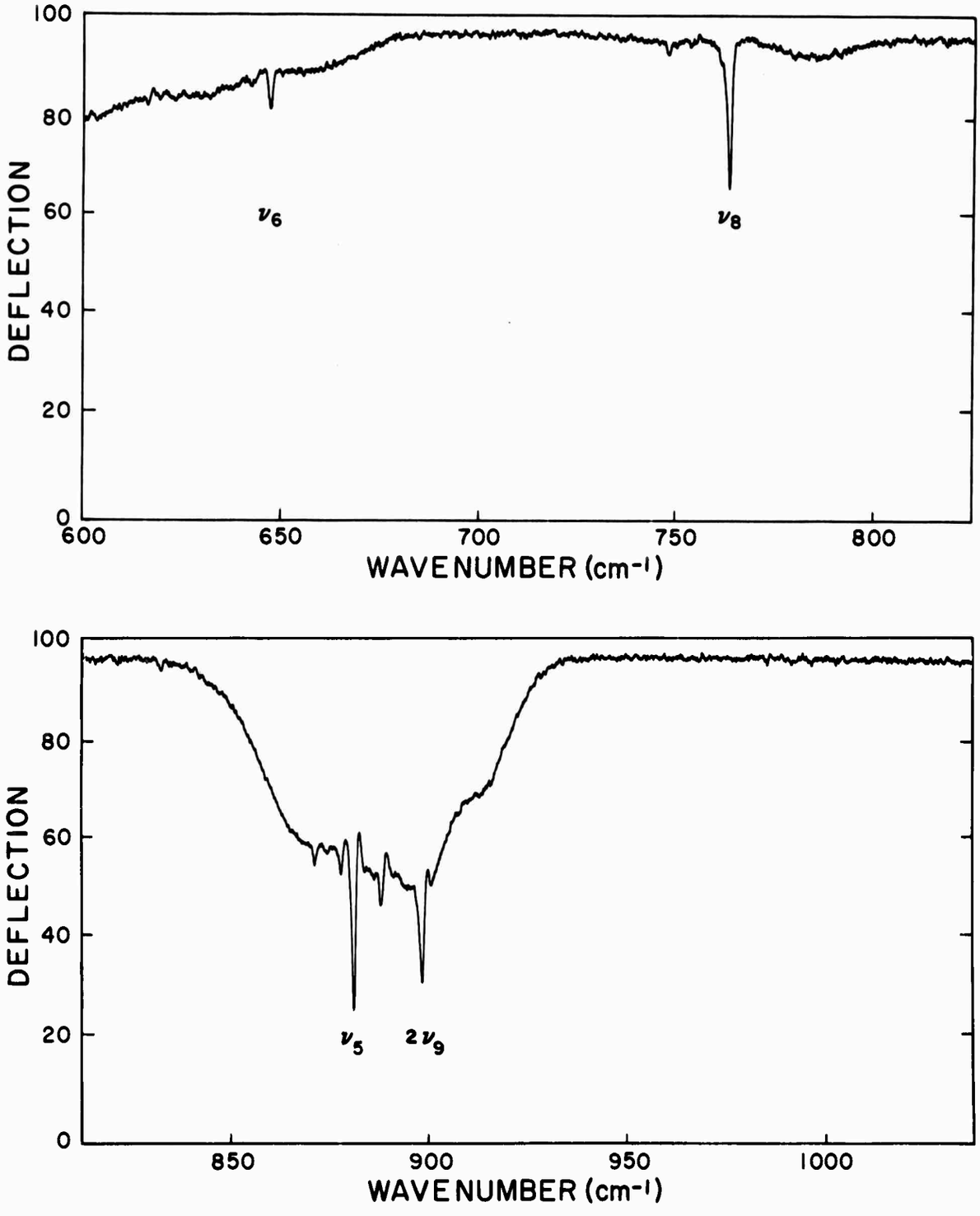

Fig. 4. Spectrum of HNO_3 vapor in the region 600-4000 cm^{-1} at ~0.5 cm^{-1} resolution, 4.6 mmHg pressure, at 40°C in the 9.94 cm glass absorption cell.

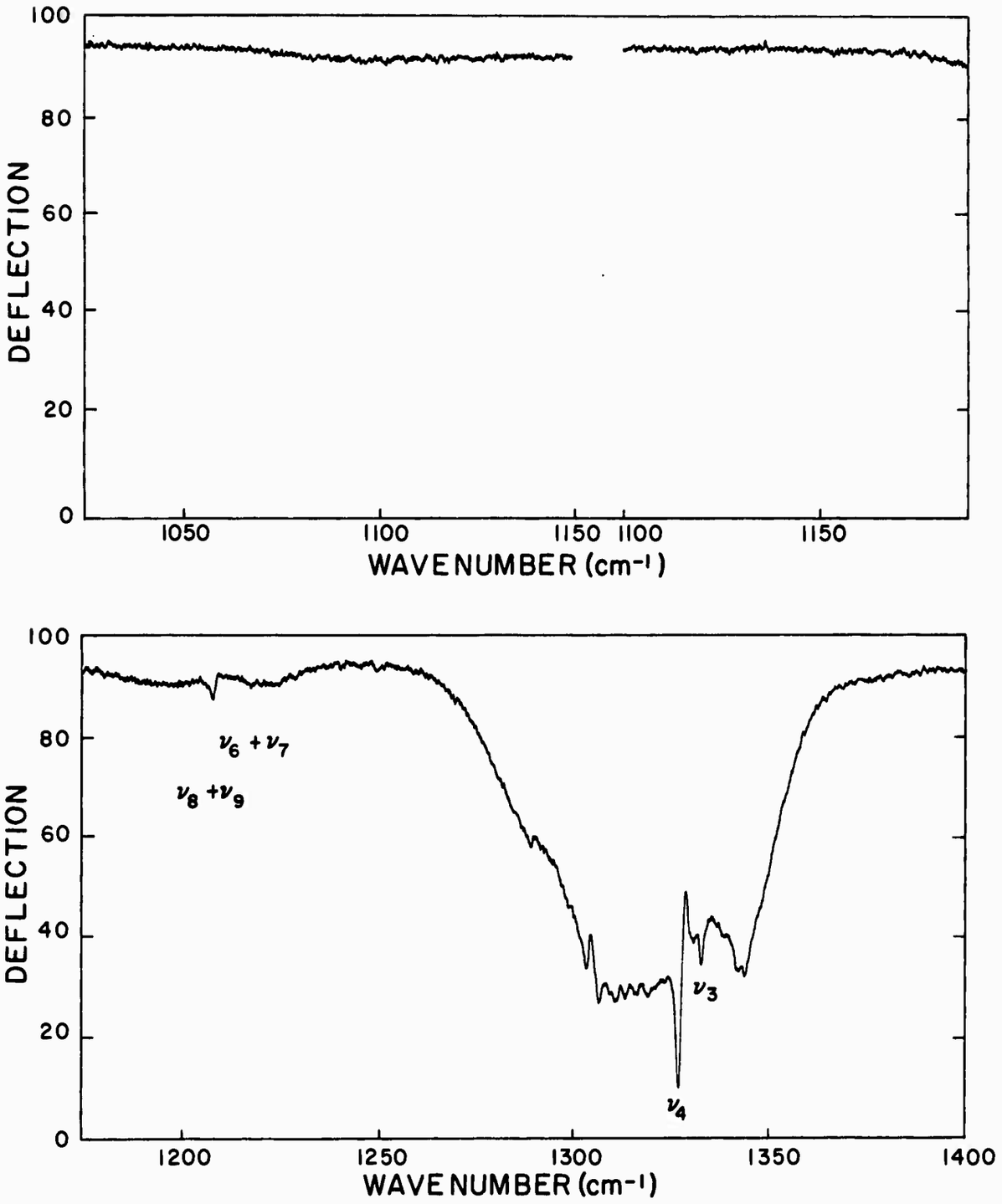
100
80
60
40
20
0
DEFLECTION
1050
1100
1150
1100
1150
WAVENUMBER (cm⁻¹)
100
80
60
40
20
0
DEFLECTION
ν6 + ν7
ν8 + ν9
ν3
ν4
1200
1250
1300
1350
1400
WAVENUMBER (cm⁻¹)

Fig. 4. Cont.

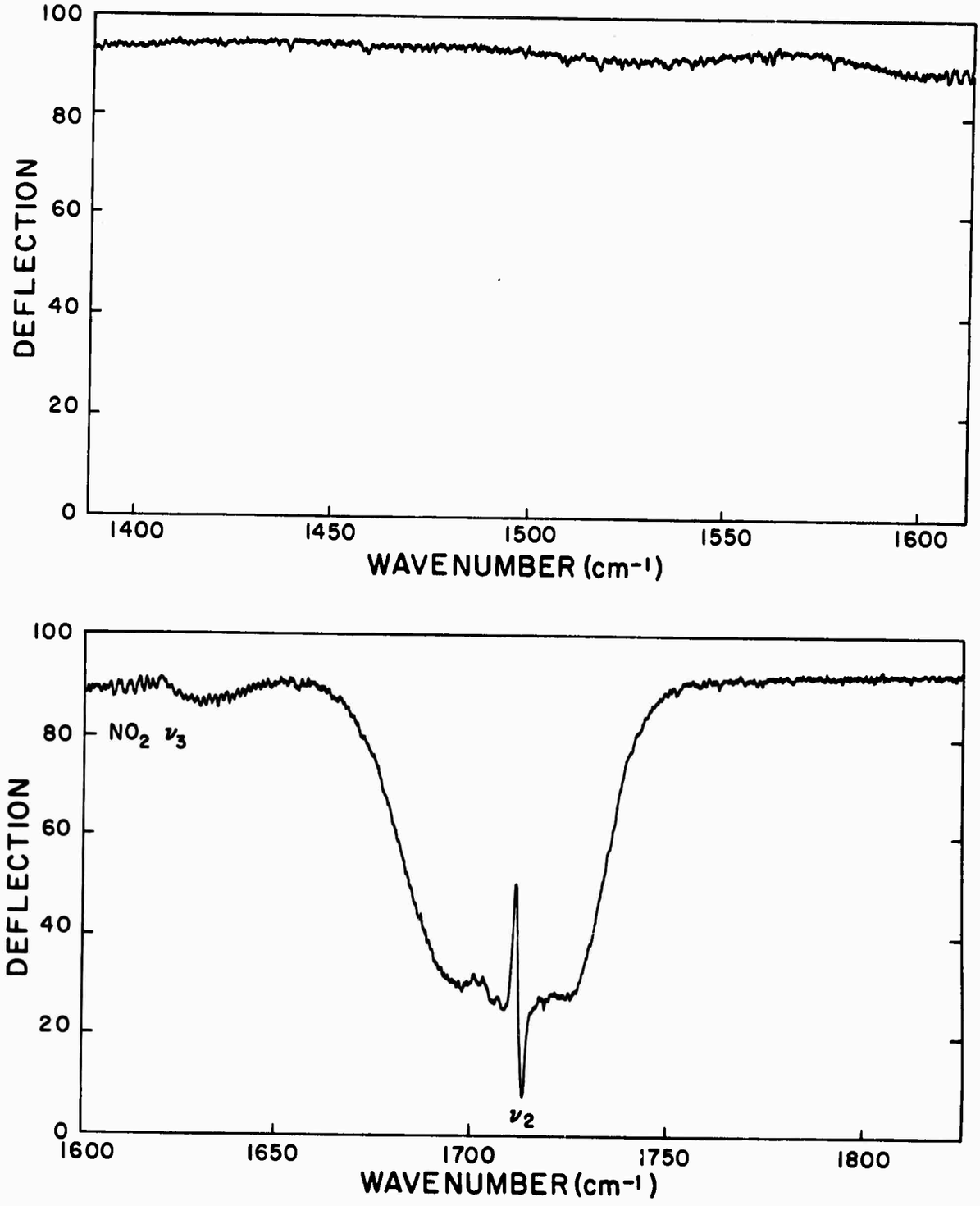
100
80
60
40
20
0
DEFLECTION
1400
1450
1500
1550
1600
WAVENUMBER (cm⁻¹)
100
80
60
40
20
0
DEFLECTION
NO2 ν3
ν2
1600
1650
1700
1750
1800
WAVENUMBER (cm⁻¹)

Fig. 4. Cont.

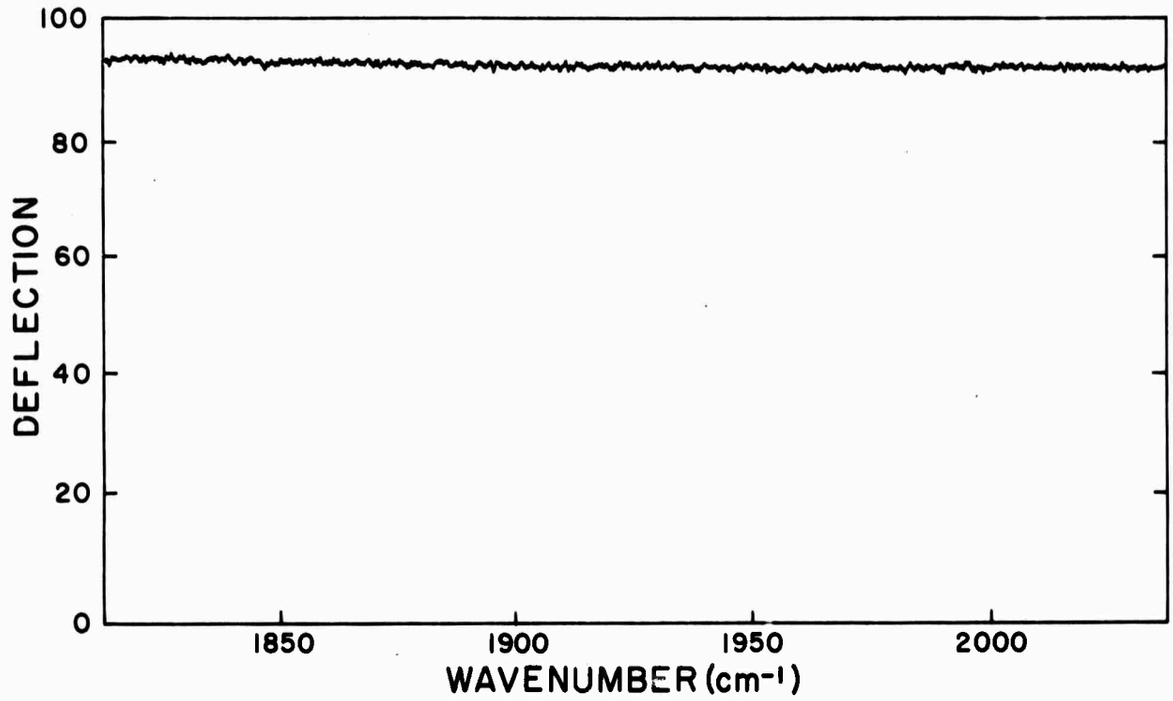
100
80
60
40
20
0
DEFLECTION
1850
1900
1950
2000
WAVENUMBER (cm⁻¹)

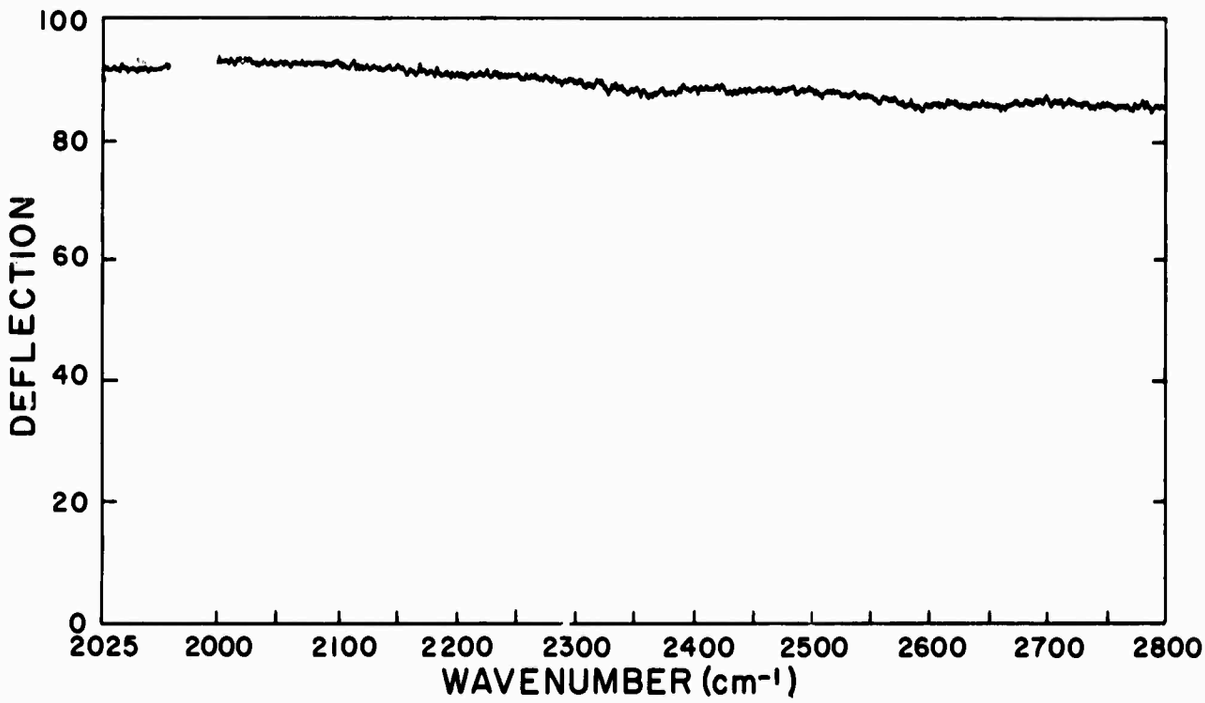
100
80
60
40
20
0
DEFLECTION
2025
2000
2100
2200
2300
2400
2500
2600
2700
2800
WAVENUMBER (cm⁻¹)

Fig. 4. Cont.

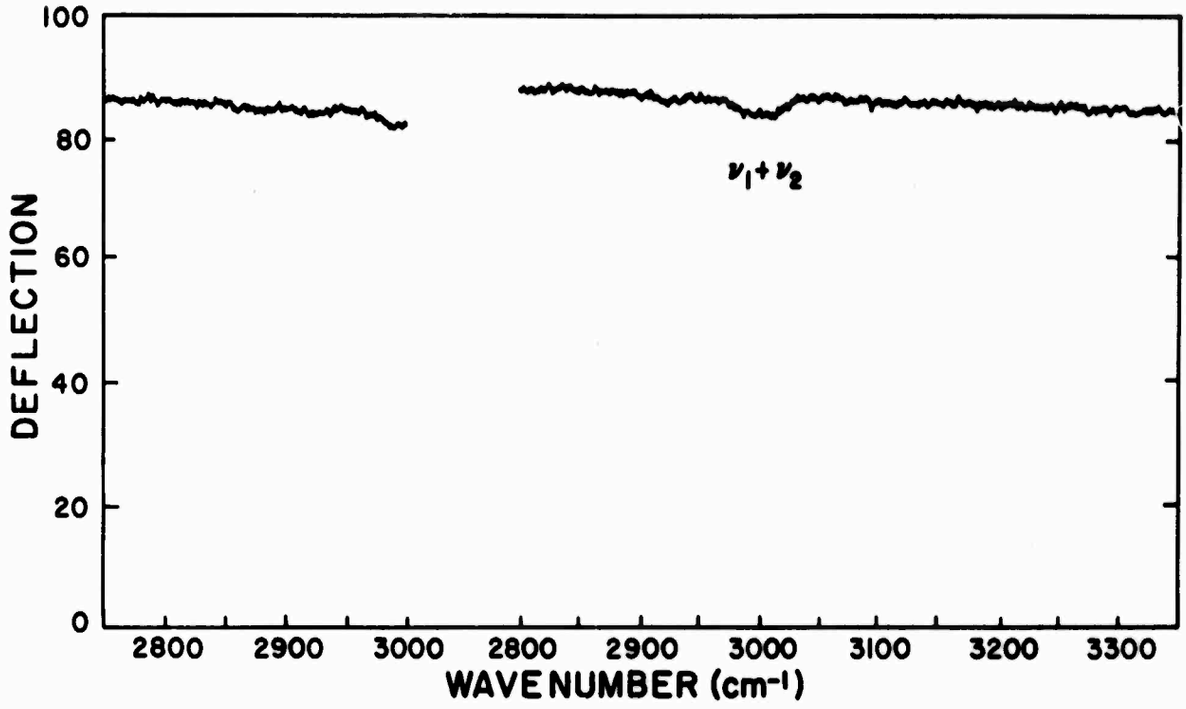
100
80
60
40
20
0
DEFLECTION
$\nu_1+\nu_2$
2800
2900
3000
2800
2900
3000
3100
3200
3300
WAVENUMBER (cm⁻¹)

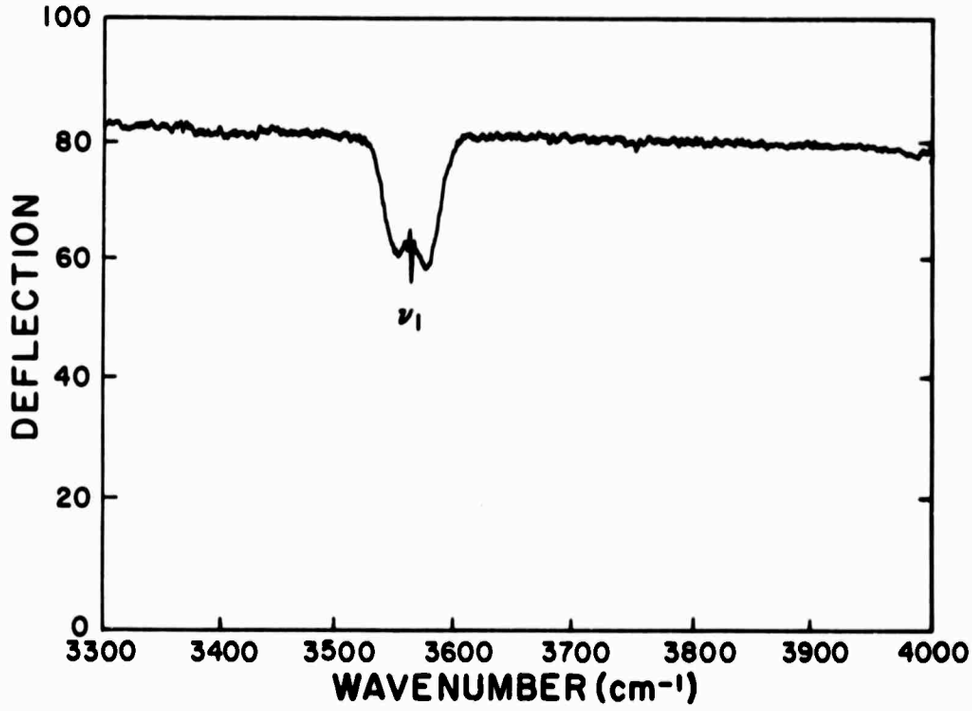
100
80
60
40
20
0
DEFLECTION
ν_1
3300
3400
3500
3600
3700
3800
3900
4000
WAVENUMBER (cm⁻¹)

Fig. 4. Cont.

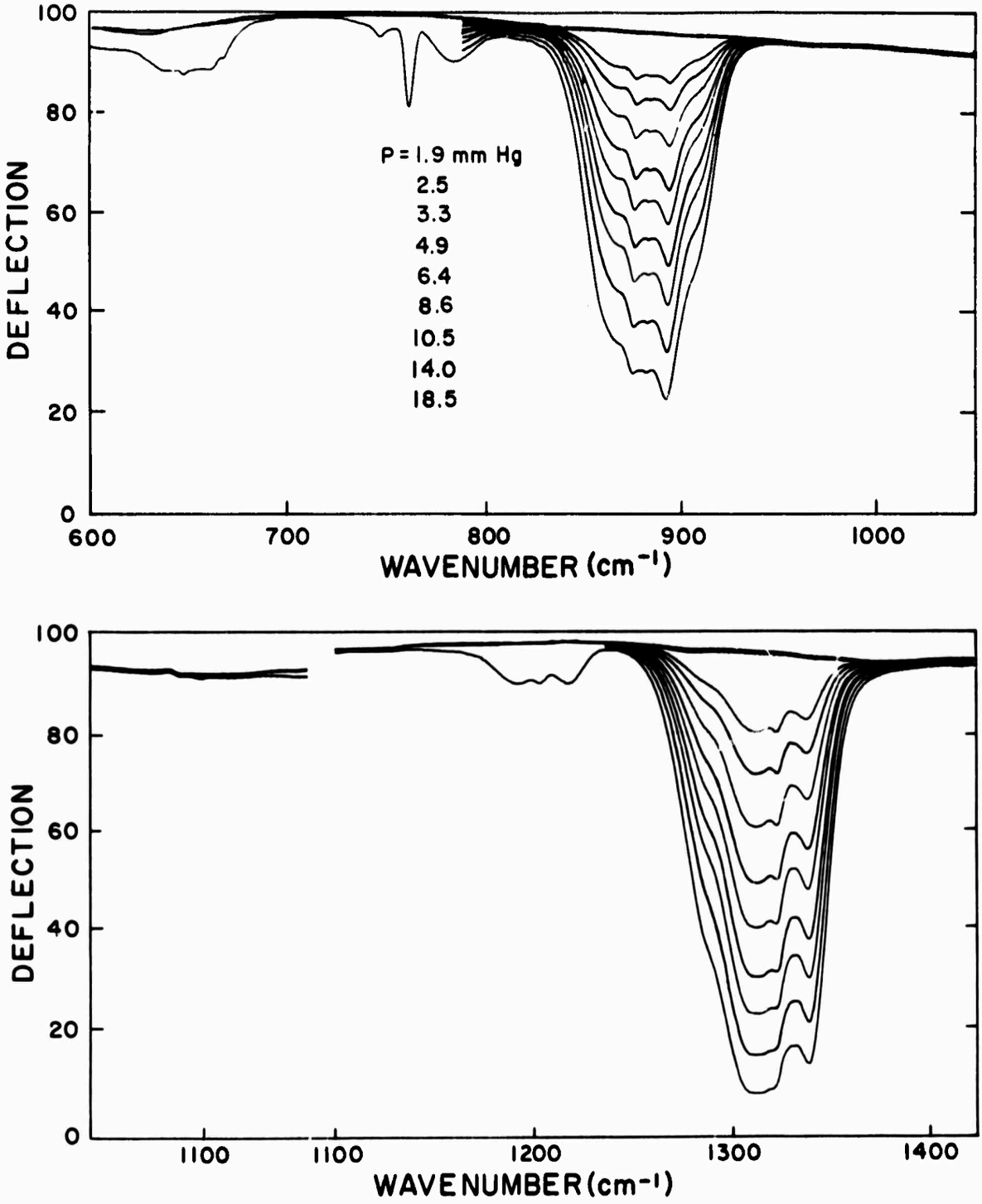

Fig. 5. Degraded spectra of HNO_3 vapor at different pressures at 40°C in the 4.93 cm glass cell.

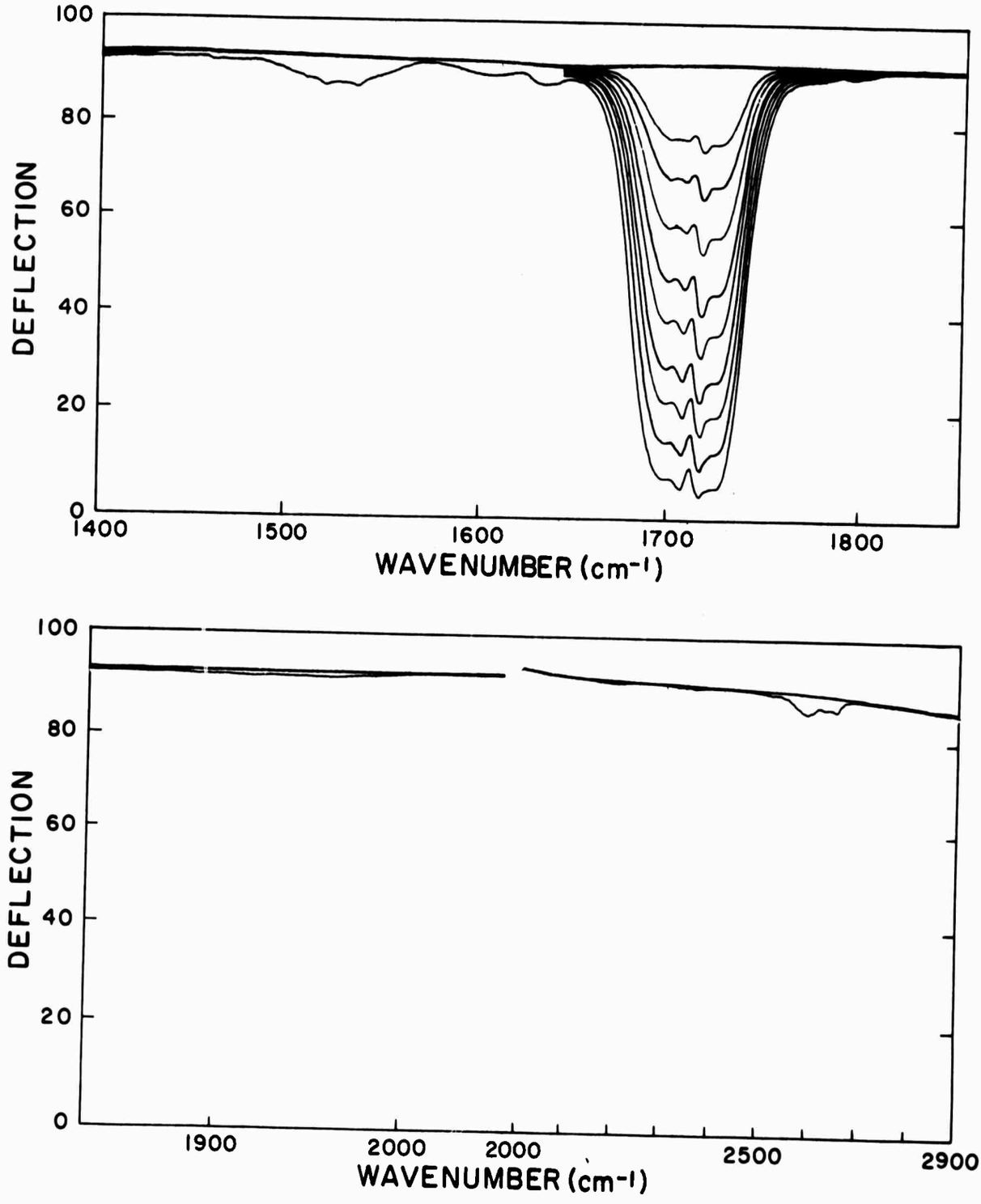
100
80
60
40
20
0
DEFLECTION
1400
1500
1600
1700
1800
WAVENUMBER (cm⁻¹)
100
80
60
40
20
0
DEFLECTION
1900
2000
2000
2500
2900
WAVENUMBER (cm⁻¹)

Fig. 5. Cont.

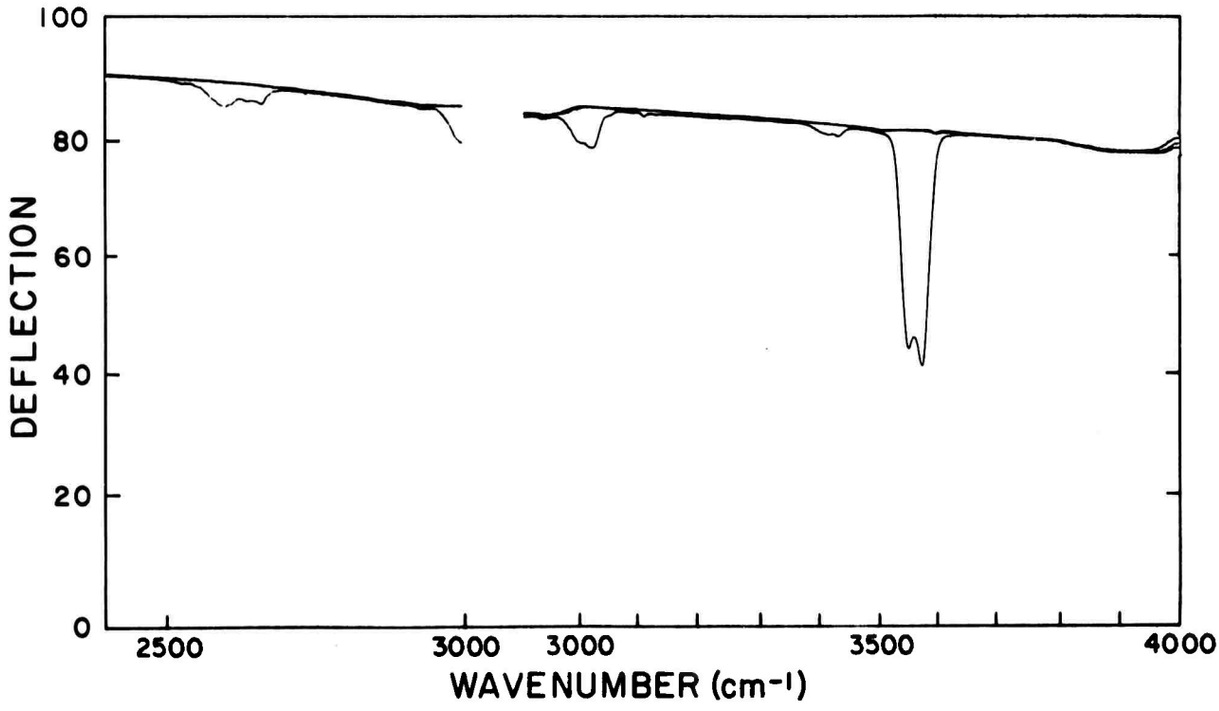
100
80
60
40
20
0
DEFLECTION
2500
3000
3000
3500
4000
WAVENUMBER (cm-1)

Fig. 5. Cont.

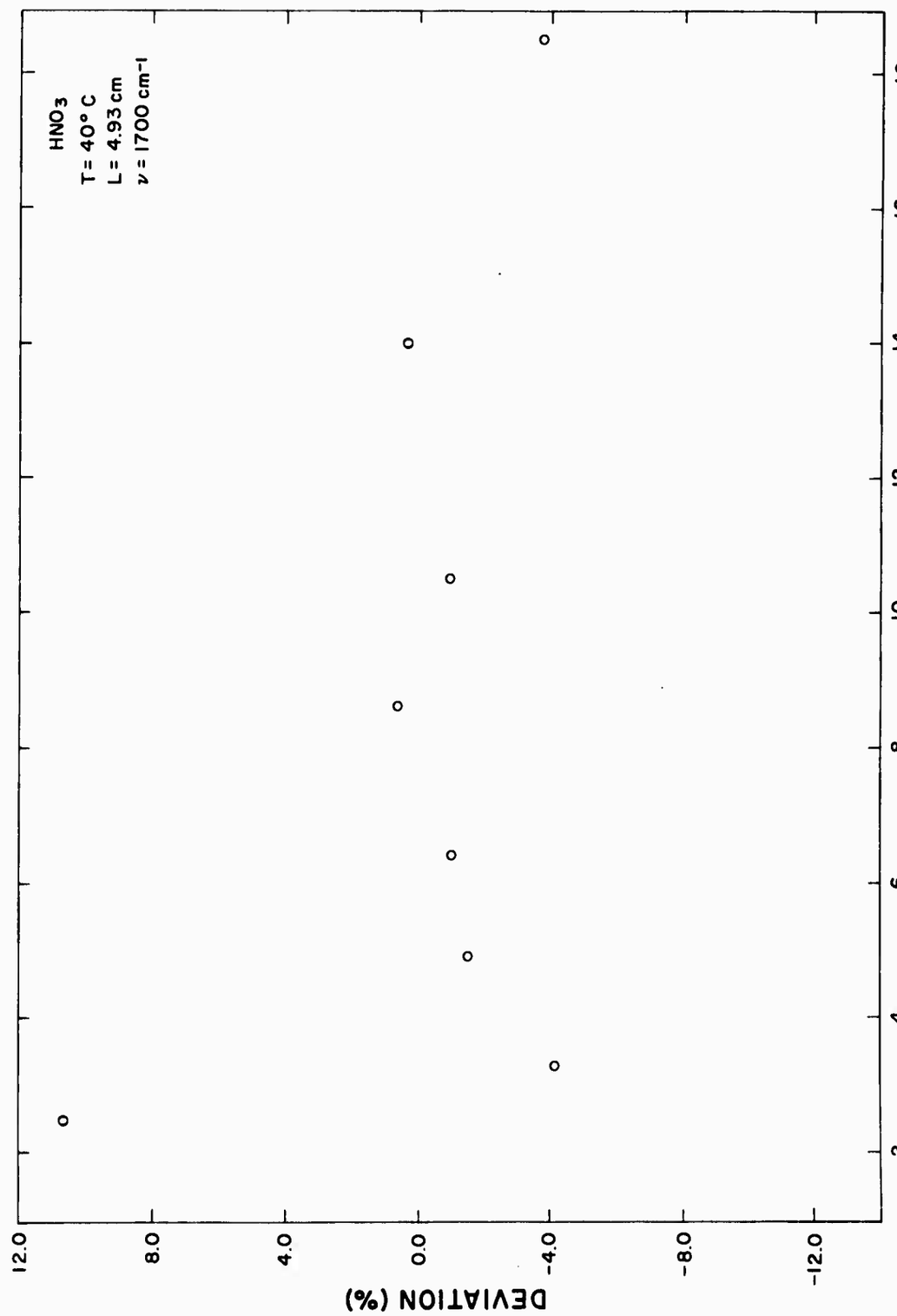

Fig. 6. A plot of the deviation of $-(\ln \bar{T}(\nu)/p$ from the average as a function of the HNO_3 pressure p for ν = 1700 cm^{-1}, at 40°C in the 4.93 cm glass cell.

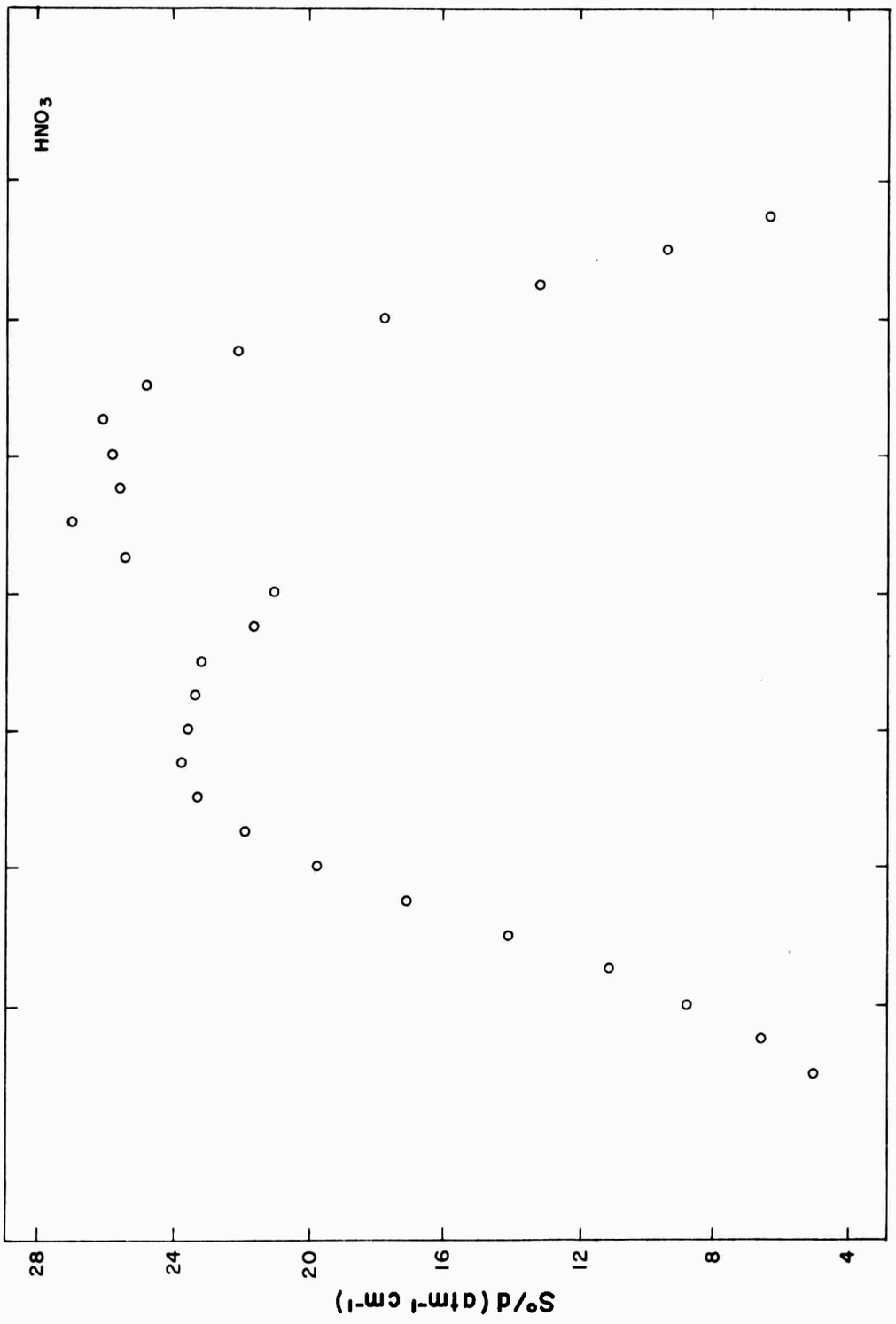

Fig. 7. Frequency dependence of the absorption coefficient $k(\nu) = S^{o}(\nu)/d(\nu)$ for the 5.9μ band of HNO_3 vapor at 40°C.

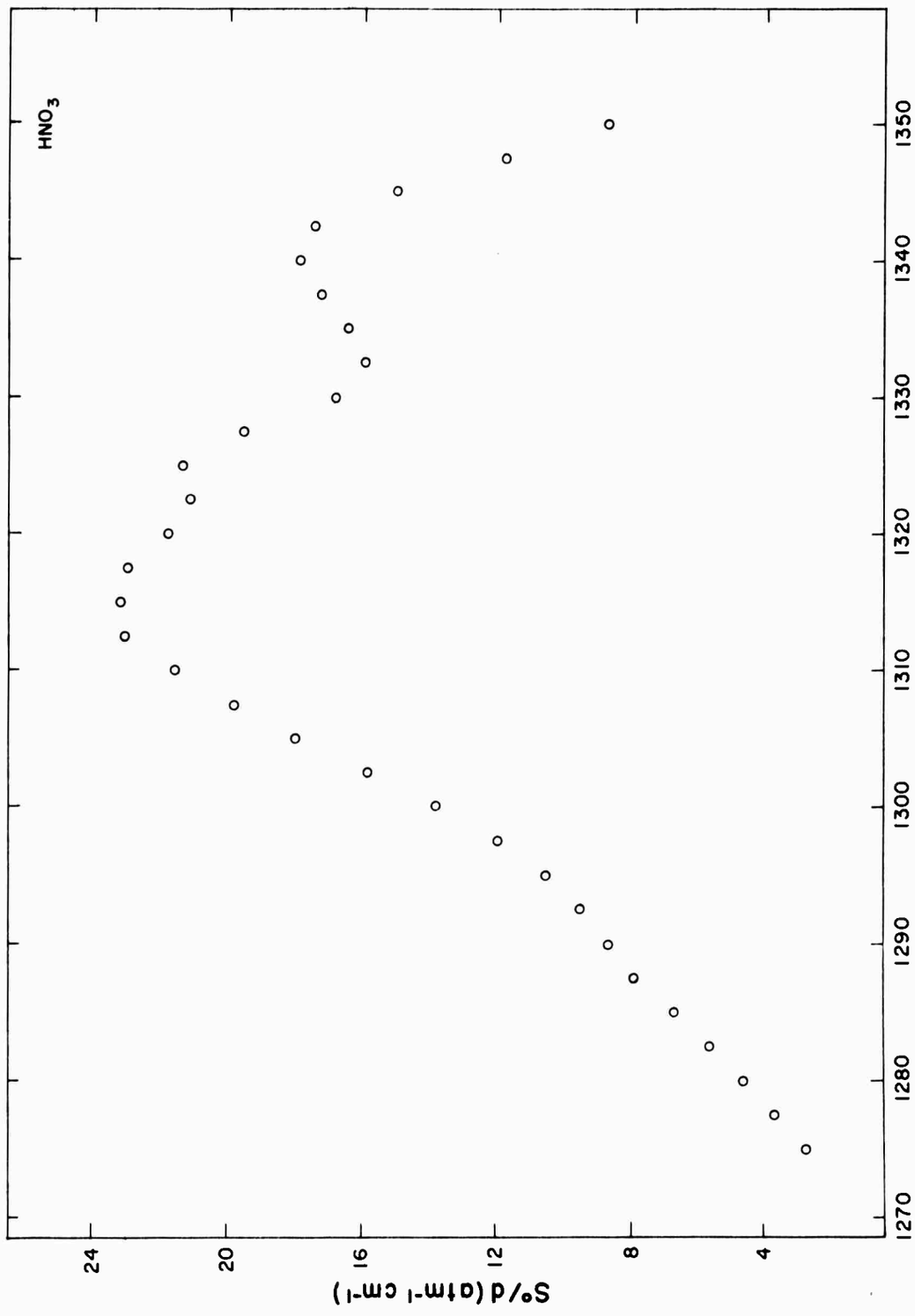

Fig. 8. Frequency dependence of the absorption coefficient $k(\nu) = S^{o}(\nu)/d(\nu)$ for the 7.5μ band of HNO_3 vapor at 40°C.

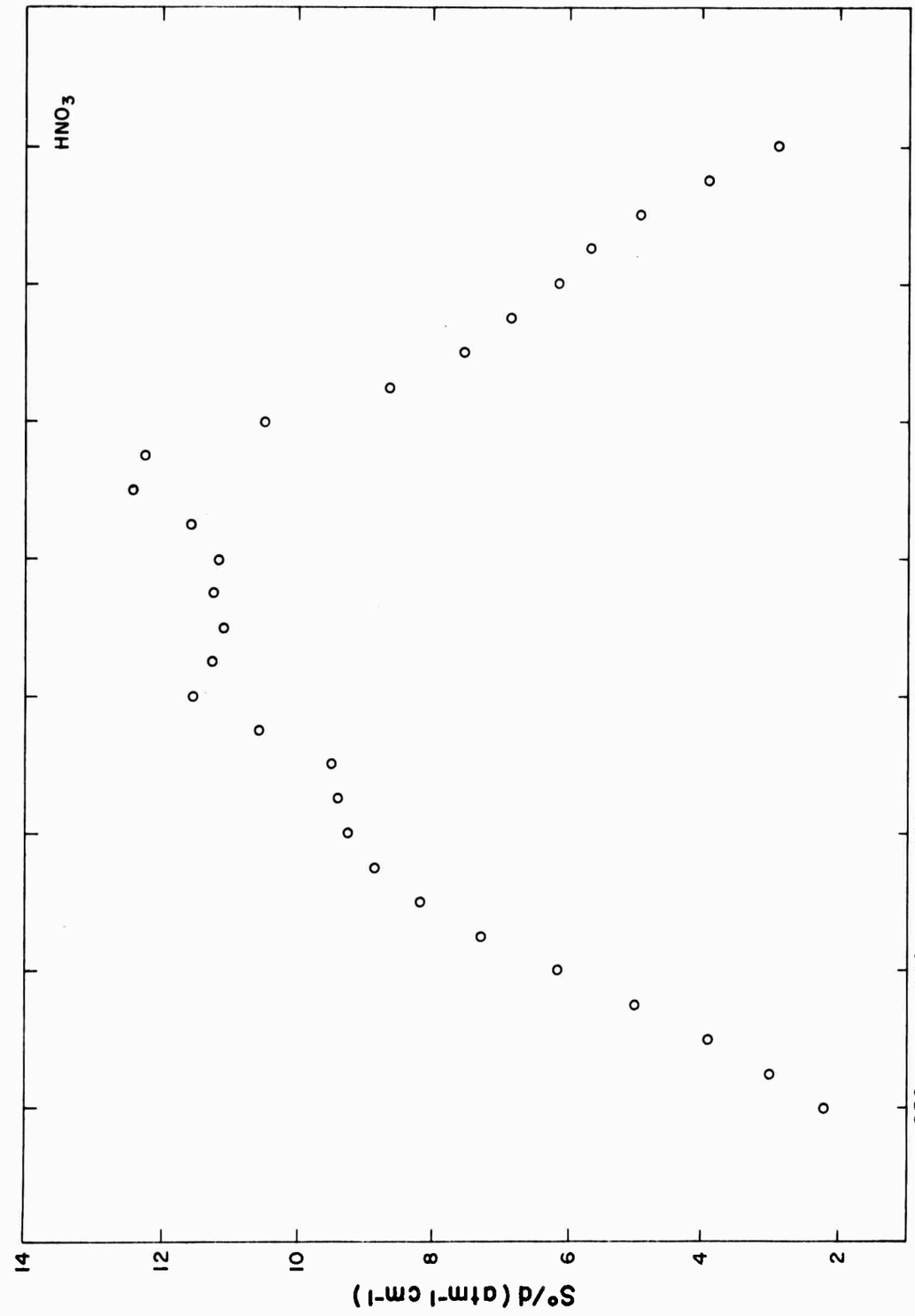

Fig. 9. Frequency dependence of the absorption coefficient $k(\nu) = S^{o}(\nu)/d(\nu)$ for the 11.3μ band of HNO_3 vapor at 40°C.

TABLE I.

ν (cm^{-1})	x/L (cm^{-1})	$2\pi\gamma^{o}/d$ (atm^{-1})	S^{o}/d ($cm^{-1}\ atm^{-1}$)
850.0	1.973@-03	1.114@+03	2.197@+00
852.5	6.446@-03	4.616@+02	2.975@+00
855.0	9.205@-03	4.249@+02	3.911@+00
857.5	1.182@-02	4.257@+02	5.032@+00
860.0	1.315@-02	4.681@+02	6.154@+00
862.5	1.574@-02	4.617@+02	7.268@+00
865.0	1.739@-02	4.686@+02	8.150@+00
867.5	1.921@-02	4.590@+02	8.817@+00
870.0	1.876@-02	4.914@+02	9.217@+00
872.5	1.923@-02	4.884@+02	9.389@+00
875.0	1.605@-02	5.896@+02	9.461@+00
877.5	1.859@-02	5.676@+02	1.055@+01
880.0	1.922@-02	6.013@+02	1.156@+01
882.5	1.987@-02	5.678@+02	1.128@+01
885.0	2.074@-02	5.351@+02	1.110@+01
887.5	2.264@-02	4.965@+02	1.124@+01
890.0	2.214@-02	5.047@+02	1.117@+01
892.5	2.145@-02	5.394@+02	1.157@+01
895.0	1.788@-02	6.936@+02	1.240@+01
897.5	1.152@-02	1.063@+03	1.224@+01
900.0	8.040@-03	1.305@+03	1.049@+01
902.5	8.517@-03	1.014@+03	8.638@+00
905.0	1.157@-02	6.487@+02	7.509@+00
907.5	1.676@-02	4.078@+02	6.835@+00
910.0	5.116@-03	1.199@+03	6.136@+00
912.5	1.217@-02	4.652@+02	5.661@+00
915.0	1.118@-02	4.383@+02	4.899@+00
917.5	8.175@-03	4.756@+02	3.888@+00
920.0	7.406@-03	3.870@+02	2.866@+00

TABLE II.

ν (cm^{-1})	x/L (cm^{-1})	$2\pi\gamma^{o}/d$ (atm^{-1})	S^{o}/d ($cm^{-1}\ atm^{-1}$)
1275.0	6.234@-03	3.435@+02	2.828@+00
1277.5	1.359@-02	2.763@+02	3.756@+00
1280.0	9.274@-03	4.972@+02	4.611@+00
1282.5	8.395@-03	6.685@+02	5.612@+00
1285.0	9.859@-03	6.852@+02	6.755@+00
1287.5	1.345@-02	5.885@+02	7.912@+00
1290.0	1.531@-02	5.720@+02	8.759@+00
1292.5	1.602@-02	5.963@+02	9.552@+00
1295.0	1.472@-02	7.138@+02	1.051@+01
1297.5	1.263@-02	9.402@+02	1.187@+01
1300.0	1.199@-02	1.146@+03	1.374@+01
1302.5	1.020@-02	1.552@+03	1.583@+01
1305.0	1.028@-02	1.751@+03	1.800@+01
1307.5	6.541@-03	3.024@+03	1.978@+01
1310.0	1.318@-02	1.633@+03	2.151@+01
1312.5	2.545@-02	9.025@+02	2.297@+01
1315.0	2.335@-02	9.891@+02	2.309@+01
1317.5	2.214@-02	1.032@+03	2.286@+01
1320.0	1.559@-02	1.391@+03	2.168@+01
1322.5	1.170@-02	1.799@+03	2.105@+01
1325.0	1.541@-02	1.383@+03	2.132@+01
1327.5	1.898@-02	1.028@+03	1.951@+01
1330.0	1.577@-02	1.067@+03	1.682@+01
1332.5	1.920@-02	8.718@+02	1.596@+01
1335.0	2.681@-02	6.124@+02	1.642@+01
1337.5	3.365@-02	5.125@+02	1.725@+01
1340.0	3.107@-02	5.149@+02	1.787@+01
1342.5	1.790@-02	9.716@+02	1.739@+01
1345.0	9.048@-03	1.846@+03	1.486@+01
1347.5	5.356@-03	2.181@+03	1.168@+01
1350.0	2.970@-03	2.934@+03	8.716@+00

TABLE III.

ν (cm^{-1})	x/L (cm^{-1})	$2\pi\gamma^{o}/d$ (atm^{-1})	S^{o}/d ($cm^{-1}\ atm^{-1}$)
1675.0	2.057@-02	2.432@+02	5.003@+00
1677.5	1.561@-02	4.266@+02	6.659@+00
1680.0	1.575@-02	5.539@+02	8.803@+00
1682.5	1.948@-02	5.769@+02	1.124@+01
1685.0	2.225@-02	6.346@+02	1.412@+01
1687.5	2.442@-02	7.017@+02	1.713@+01
1690.0	2.779@-02	7.135@+02	1.983@+01
1692.5	2.906@-02	7.550@+02	2.194@+01
1695.0	3.159@-02	7.381@+02	2.331@+01
1697.5	3.501@-02	6.807@+02	2.383@+01
1700.0	3.264@-02	7.223@+02	2.358@+01
1702.5	2.353@-02	9.955@+02	2.342@+01
1705.0	1.050@-02	2.212@+03	2.322@+01
1707.5	1.617@-02	1.340@+03	2.167@+01
1710.0	1.580@-02	1.329@+03	2.109@+01
1712.5	1.648@-02	1.546@+03	2.547@+01
1715.0	1.962@-02	1.375@+03	2.699@+01
1717.5	2.704@-02	9.460@+02	2.558@+01
1720.0	3.200@-02	8.075@+02	2.588@+01
1722.5	3.421@-02	7.615@+02	2.605@+01
1725.0	3.205@-02	7.735@+02	2.479@+01
1727.5	3.482@-02	6.361@+02	2.215@+01
1730.0	3.205@-02	5.515@+02	1.768@+01
1732.5	2.962@-02	4.458@+02	1.320@+01
1735.0	4.170@-02	2.259@+02	9.420@+00
1737.5	4.491@-02	1.402@+02	6.296@+00

TABLE V. Integrated Intensities for HNO_3 at 40°C

Region (cm^{-1})	$S_b^{o(a)}$ (cm^{-2} atm^{-1})	$S_b^{o(b)}$ (cm^{-2} atm^{-1})
950.0-920.0	582 ± 10%	609 ± 5%
1275.0-1350.0	1126 ± 10%	1186 ± 5%
1675.0-1737.5	1221 ± 10%	1254 ± 5%

$$S_b^{o(a)} = \int_{\nu_1}^{\nu_2} (S^o(\nu)/d(\nu))d\nu$$

$$S_b^{o(b)} = \frac{-1}{pL} \int_{\nu_1}^{\nu_2} (\ell n\, \bar{T}(\nu))d\nu \text{ from short cell.}$$

TABLE IV. Derivation of Band-Model Parameters for $\nu = 1700\ cm^{-1}$

L (cm)	y_j Observed (atm^{-1})		y_j Fitted (atm^{-1})				Error (%)			
	a	b	a1	a2	a3	b	a1	a2	a3	b
1.020	24.54	23.32	23.29	23.80	23.76	22.24	5.3	3.0	3.2	4.8
2.028	44.58	46.81	44.94	45.66	45.44	43.46	0.8	2.4	1.9	7.7
4.930	97.17	92.31	101.1	101.4	100.7	100.8	3.9	4.3	3.6	8.4
9.940	185.2	194.4	182.5	180.2	180.2	189.2	1.5	2.7	2.7	2.7

Case	x/L (cm^{-1})	$2\pi\gamma^o/d$ (atm^{-1})	S^o/d ($cm^{-1}\ atm^{-1}$)
a1	0.03264	722.3	23.58
a2	0.03984	609.1	24.27
a3	0.02320	1049.	24.35
b	0.01817	1222.	22.20

a. y_j as obtained from the data.

b. Change of +5% in points y_1, y_3, -5% in points y_2, y_4.

a1. Exponential intensity distribution according to Eq.(6); least squares according to Eq.(10).

a2. Exponential intensity distribution according to Eq.(6); iteration calculation according to Eq.(11)-(13).

a3. S^{-1} Tailed exponential intensity according to Eq.(7); iteration calculation according to Eq.(11)-(13).

Unclassified

Security Classification

DOCUMENT CONTROL DATA - R & D

(Security classification of title, body of abstract and indexing annotation must be entered when the overall report is classified)

1. ORIGINATING ACTIVITY (Corporate author)
University of Denver
Department of Physics
Denver, Colorado 80210

2a. REPORT SECURITY CLASSIFICATION
Unclassified

2b. GROUP

3. REPORT TITLE
STATISTICAL BAND MODEL PARAMETERS AND INTEGRATED INTENSITIES FOR THE 5.9μ, 7.5μ, AND 11.3μ BANDS OF HNO_3 VAPOR

4. DESCRIPTIVE NOTES (Type of report and inclusive dates)
Scientific. Interim.

5. AUTHOR(S) (First name, middle initial, last name)
Aharon Goldman
Thomas G. Kyle
Francis G. Bonomo

6. REPORT DATE
January 1970

7a. TOTAL NO. OF PAGES
47

7b. NO. OF REFS
11

8a. CONTRACT OR GRANT NO. ARPA ORDER No. 363
F19628- 8-C-0233

b. PROJECT, Task, Work Unit Nos.
8662 - n/2 - n/2

c. Dod Element: 6250301D

d. Dod Subelement: n/a

9a. ORIGINATOR'S REPORT NUMBER(S)
SCIENTIFIC REPORT NO. 7

9b. OTHER REPORT NO(S) (Any other numbers that may be assigned this report)
AFCRL-70-0091

10. DISTRIBUTION STATEMENT
This document has been approved for public release and sale; its distribution is unlimited.

11. SUPPLEMENTARY NOTES
This research was supported by the Advanced Research Projects Agency

12. SPONSORING MILITARY ACTIVITY
Air Force Cambridge Research Laboratories (CRO)
L. G. Hanscom Field
Bedford, Massachusetts 01730

13. ABSTRACT

Quantitative absorption measurements of the 5.9μ, 7.5μ and the 11.3μ bands of pure HNO_3 vapor were carried out at 40°C. Use was made of absorption cells of various lengths in order to obtain curves of growth. The statistical spectral band model was applied and band model parameters and integrated intensities were derived.

DD FORM 1 NOV 65 1473

Unclassified

Security Classification

14. KEY WORDS	LINK A		LINK B		LINK C	
	ROLE	WT	ROLE	WT	ROLE	WT
Infrared Spectra						
Statistical Band Model						
HNO_3						